IOPscience iopscience.iop.org

Home Search Collections Journals About Contact us My IOPscience

Atomic and electronic structures of a-SiC:H from tight-binding molecular dynamics

This article has been downloaded from IOPscience. Please scroll down to see the full text article.

2003 J. Phys.: Condens. Matter 15 4119

(http://iopscience.iop.org/0953-8984/15/24/305)

View the table of contents for this issue, or go to the journal homepage for more

Download details:
IP Address: 171.66.16.121
The article was downloaded on 19/05/2010 at 12:18

Please note that terms and conditions apply.

INSTITUTE OF PHYSICS PUBLISHING JOURNAL OF PHYSICS: CONDENSED MATTER

J. Phys.: Condens. Matter **15** (2003) 4119–4126 PII: S0953-8984(03)61686-3

Atomic and electronic structures of a-SiC:H from tight-binding molecular dynamics

V I Ivashchenko[1], **P E A Turchi**[2], **V I Shevchenko**[1,3], **L A Ivashchenko**[1] **and G V Rusakov**[1]

[1] Institute of Problems of Materials Science, NAS of Ukraine, Krzhyzhanovsky Street 3, 03142 Kyiv, Ukraine
[2] Lawrence Livermore National Laboratory (L-353), PO Box 808, Livermore, CA 94551, USA

E-mail: shev@materials.kiev.ua

Received 3 April 2003
Published 6 June 2003
Online at stacks.iop.org/JPhysCM/15/4119

Abstract

The atomic and electronic properties of amorphous unhydrogenated (a-SiC) and hydrogenated (a-SiC:H) silicon carbides are studied using an $sp^3s^\star$ tight-binding force model with molecular dynamics simulations. The parameters of a repulsive pairwise potential are determined from *ab initio* pseudopotential calculations. Both carbides are generated from dilute vapours condensed from high temperature, with post-annealing at low temperature for a-SiC:H. A plausible model for the inter-atomic correlations and electronic states in a-SiC:H is suggested. According to this model, the formation of the amorphous network is weakly sensitive to the presence of hydrogen. Hydrogen passivates effectively only the weak bonds of threefold-coordinated atoms. Chemical ordering is very much affected by the cooling rate and the structure of the high-temperature vapour. The as-computed characteristics are in rather good agreement with the results for a-SiC and a-Si:H from *ab initio* calculations.

1. Introduction

Hydrogenated amorphous silicon carbide (a-SiC:H) layers are widely used as window coatings in high-efficiency amorphous solar cells, and in other applications as well, such as in light-emitting diodes, colour sensors, electrophotography devices, and phototransistors [1, 2]. Optoelectronic characteristics of a-SiC:H are very sensitive to hydrogen concentration, preparation conditions, and precursors [3]. It is well known [1–3] that only hydrogenated silicon carbide is appropriate for use in semiconductor devices. Much effort has been devoted to the study of its structural properties as reported in previous studies [1, 3–5]. Here we single out the experimental findings that directly relate to this work. Amorphous hydrogenated SiC

[3] Author to whom any correspondence should be addressed.

is often viewed as a tetrahedral network that has predominantly heteronuclear bonding with a small fraction of Si–Si and C–C bonds. On the other hand, some authors describe a-SiC:H as chemically disordered, with both homonuclear and heteronuclear bonds. Besides, sp^2 carbon atoms, constituting polymer-like networks with C=C bonds, were also revealed in a-SiC:H amorphous networks. It is well known that hydrogen is able to create different $C–H_n$ groups and preferentially surrounds the carbon atoms, while, among $Si–H_n$ groups, Si–H bonds are frequently identified [6]. Hydrogen addition to a reactive gas promotes the formation of Si–C bonds [7], and its effect on the strengthening properties of amorphous tetragonal networks has already been mentioned [5]. The hydrogenated samples undergo intense hydrogen effusion in the 400–600 °C temperature range [6, 8].

The state of affairs on theoretical investigations of a-SiC was reported in [9, 10]. In summary, the structural, dynamical, and electronic properties of a-SiC were studied by using molecular dynamics (MD) simulations based on a pseudopotential approach (PA) within the local density approximation (LDA), a combined empirical potential (EP)–Monte Carlo (MC) method, EP–MD simulations based on the EP of Tersoff, and tight-binding (TB)–MD calculations. The resulting PA–LDA densities of states (DOS) did not show a distinct semiconducting band gap (BG), though the DOS of the 54-atom sample [4] had a distinct dip demonstrating the trend towards gap formation. It is worth noting that although PA–LDA can be used appropriately to describe the atomic distribution in a-SiC, the electronic states are incorrectly computed, because the LDA is known to underestimate the BG [11]. Since one of our objectives was to examine the DOS in the band gap region, we have chosen a TB model that is able to correctly reproduce the semiconducting band gap in the materials under investigation.

2. Computational aspects

In this work we use a procedure based on the orthogonal $sp^3s^\star$ tight-binding model [11] to determine the atomic and electronic structures of large-sized samples of a-SiC and a-SiC:H under conditions close to experimental ones. The repulsive contributions not included in the TB calculation and needed for performing MD simulations were considered in the form suggested by the authors [12]:

$$V(r) = U_1 \exp\left(-\frac{r - r_0}{\alpha}\right) + U_2 \frac{r_0}{r}, \tag{1}$$

where r is the distance between neighbouring atoms, r_0 is its equilibrium counterpart in the ZnS phase, and U_1, U_2, and α are the parameters defined for Si–S, Si–C, C–C, Si–H, C–H, and H–H pairs.

The parameters of the repulsive pairwise potentials were determined from total energy calculations carried out for c-Si, c-C, and c-SiC in the rock-salt and diamond-like structures, and for hypothetical β-SiH, β-CH (like β-SiC), and bcc H with different locations of the basis atoms using a first-principles PA as described in [13]. We used norm-conserving pseudopotentials constructed according to the scheme of Hamann and represented in the fully separable form. The Brillouin zone (BZ) integration over k-points is replaced by a sum over a set of ten special k-points according to the Monkhorst–Pack scheme. The Kohn–Sham plane-wave basis set was truncated beyond an energy of 35 Ryd. The exchange–correlation energy was considered in the LDA. Using this approach, we obtained the following bond lengths (in Å): 2.34 (2.35 [11]), 1.564 (1.54 [11]), 1.89 (1.89 [11]), 1.519 (1.520 [14]), 1.125 (1.120 [15]), and 0.782 (0.741 [15]) for Si–Si, C–C, Si–C, Si–H, C–H, and H–H bonds, respectively. The close agreement between the calculated bond lengths and their experimental counterparts (as indicated in parentheses) validates to some extent our computational scheme.

Table 1. Tight-binding parameters (eV), cut-off distances R_{cut} (Å), and potential parameters (see equation (1)), r_0 (Å), U_1 (eV), α (Å) for H–H, H–C, and H–Si pairs. For this system, $U_2 = 0$ eV.

	$E_{\mathrm{s}}^{\mathrm{H}}$	$E_{\mathrm{s}^\star}^{\mathrm{H}}$	$\mathrm{s^H s}\sigma$	$\mathrm{s^H p}\sigma$	$\mathrm{s^{\star H} p}\sigma$	R_{cut}	r_0	U_1	α
H–H	−3.400	14.000	−6.059			1.000	0.782	6.258	0.202
H–C			−6.103	−7.886	−3.493	1.550	1.125	10.861	0.307
H–Si			−3.035	−3.318		1.800	1.520	2.692	0.267

The parameters of the $\mathrm{sp^3s^\star}$-TB scheme for diamond, 3C–SiC, and c-Si and the Si–Si, Si–C, and C–C pairs of the repulsive potential (1) were carefully determined in [9, 10]. Therefore, here we only mention that our scheme gives a BG of 5.5, 1.17, and 2.4 eV for c-C, c-Si and 3C–SiC, respectively, in agreement with experiment. The Si–H, C–H, and H–H integrals were taken from [16, 17]. The form of the variation of the two-centre hopping parameters with inter-atomic distance was chosen according to the Harrison rule. The tight-binding and repulsive potential parameters for C–H, Si–H, and H–H pairs are summarized in table 1.

The NPT and NVT ensembles were considered during MD simulations of the condensed vapours and the amorphous structures, respectively. The equations of atomic motion were integrated using a velocity-Verlet algorithm. Periodic boundary conditions were applied to supercells of 128 atoms. First we generated the dilute vapour phases. For this, we initially considered cubic cells of 128 atoms (64 Si atoms and 64 C atoms for a-SiC; 58 Si atoms, 58 C atoms, and 12 H atoms for a-SiC:H) with a lattice parameter which is 1.5 times larger than that of the 3C-SiC crystal. The cubic cells contained randomly distributed atoms far apart from each other, and they were allowed to slowly shrink for about 2 ps under applied pressure at 1900 and 800 K for a-SiC and a-SiC:H, respectively. One carbon atom and one hydrogen atom in the condensed non-equilibrated a-SiC:H vapour turned out not to be bonded to any another atoms, and therefore before equilibrating they were excluded from further simulations. The fully equilibrated high-temperature structures with the density equal to that of the 3C-SiC crystal were quenched with an average cooling rate of $\sim 10^{15}$ K s^{-1} to 300 K. We applied different time steps (h) depending on sample type. In obtaining the condensed vapours and the amorphous samples, h was $\sim 10^{-14}$ and $\sim 10^{-15}$ s, respectively. Despite the use of comparatively large time steps, the MD process was stable—the potential energy variation did not exceed 5–10 meV/atom. The generated amorphous samples were then averaged for about 2 ps to get the thermal equilibrium properties. To reduce the strain, the resulting amorphous hydrogenated sample was equilibrated for 1.5 ps at 650 K and was then cooled back to 300 K. In generating the hydrogenated sample the temperature of the vapour condensation did not exceed that of hydrogen effusion. This is the important peculiarity, which essentially distinguishes our procedure from previous preparation techniques applied to a-Si:H [18, 19] and a-C:H [20].

The DOS during TB–MD simulations was computed at the centre of the BZ. An analysis of the local DOS was carried out in the framework of the recursion method (RM) of Haydock *et al* [21], and Nex [22]. The details of the calculations based on the RM and applied to compounds such as 3C-SiC are given in [9].

3. Results and discussion

In figure 1, we show the calculated partial pair-correlation functions (PCF) of a-SiC and a-SiC:H. For comparison, we also present the PCF of a 54-atom a-SiC sample [4]. The H–H

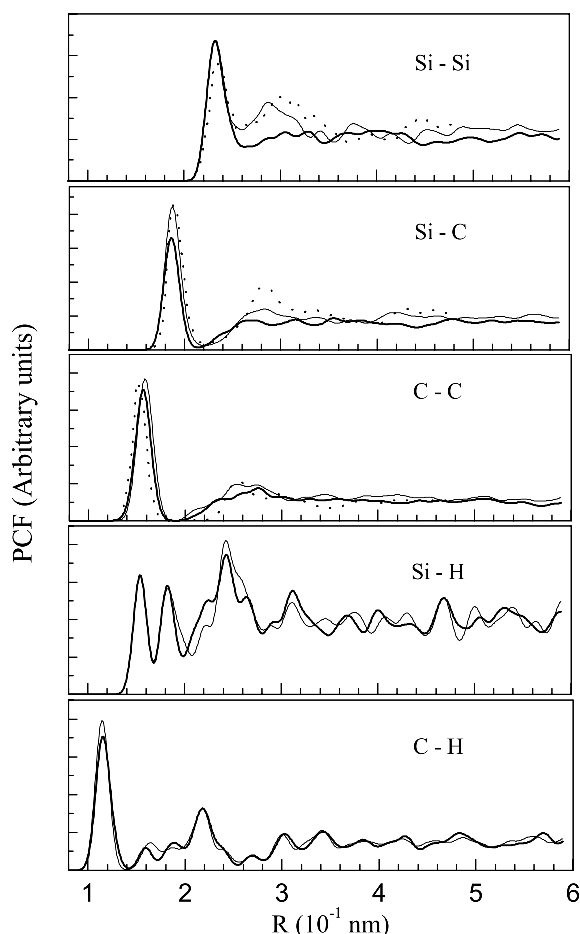

Figure 1. The partial PCF of a-SiC (thin curve) and as-quenched a-SiC:H (solid curve). For comparison, the PCF of a 54-atom a-SiC [4] (dashed curve) and pair Si–H and C–H correlations of annealed a-SiC:H (thin curve) are also presented.

partial PCF is not shown, since the statistics is very poor, owing to the very limited number of H in the a-SiC:H sample. We find a rather good agreement between our curves and the curves determined by using the PA–MD simulations. However, the first peak of C–C correlations in our spectrum is located at higher distance than that in the PA–MD spectrum, and this can be attributed to a slight overestimation of the lattice parameter of diamond predicted from our PA. Besides, the peaks of the second-neighbour interactions in our spectra are broader than in the PA–MD spectra. It is worth noting that a-SiC and a-SiC:H alloys contain about 82.0 and 64.3% fourfold-coordinated atoms, respectively. Hence, the unhydrogenated sample is less disordered than the hydrogenated one. However, this cannot be unambiguously attributed to hydrogenation, since the condensation temperature of the a-SiC:H vapour was lower than that of the unhydrogenated vapour. The positions of the corresponding peaks of the nearest-neighbour correlations in the unhydrogenated and hydrogenated samples practically coincide. The peak positions (in Å) in the case of a-SiC:H are 2.334, 1.565, 1.860, 1.538, 1.154, and 1.502 for Si–Si, C–C, Si–C, Si–H, C–H, and H–H pairs, respectively. A small difference in the peak positions in the PCF of a-SiC and a-SiC:H is observed for C–C and Si–C pairs, which

is attributed to the influence of the hydrogen atoms which preferentially surround the carbon atoms in forming C–H_n bonds. For comparison, the first Si–H and C–H peaks in the PCF of a-Si:H [19] and a-C:H [20] are located around 1.6 and 1.1–1.2 Å, respectively.

We found in a-SiC:H 5(2) H atoms participating in C–H(C–H_2) bonds. Only Si–H monohydrides are formed as a result of the interaction of 4 H atoms with the Si atoms. All the H atoms are singly bonded to Si and C atoms. Correspondingly, the average Si–H and C–H coordination is unity, i.e., not a single Si–H–Si or C–H–C bridge has been observed at the Si–H and C–H cut-off distances equal to 1.8 and 1.55 Å, respectively. The introduction of H atoms leads to an enhancement of the diffusion in the second-neighbour distribution of the Si atoms (figure 1). The analysis of the C–H PCF shows that the distribution of hydrogen around the carbon atoms in a-SiC:H resembles that in the high-density a-C:H [20], i.e., the peaks of the nearest C–H pairs around 1.154 Å are distinctly shown in the corresponding PCF. In the case of Si–H correlations, the Si–H nearest-neighbour correlation has a peak around 1.54 Å mostly owing to the formation of monohydride groups, as in a-Si:H [18, 19]. However, the C–H and Si–H correlations in a-SiC:H differ from those in a-C:H and a-Si:H because of the presence of the additional peaks associated with C–H (around 1.6 Å) and Si–H (around 1.8 Å) correlations in the PCF of a-SiC:H. The additional minor Si–H and C–H peaks were found to originate from different H–Si–C and H–C–Si configurations, respectively.

The Si–Si, Si–C, and C–C PCF of the annealed sample practically coincide with those of the as-quenched sample (not shown). More appreciable changes are observed in the Si–H and C–H pair correlations, where the first corresponding peaks become more sharply defined (figure 1). If in the as-quenched sample, a small fraction of weak Si–H and C–H bonds was revealed (the bonds which can form H–Si–H and H–C–H bridge configurations, with a small increase in their length), fewer such bonds were observed in the annealed sample. This reflects the fact that unstable configurations were annealed out, and that now only well-defined Si–H monohydride groups are present in the sample. The annealing also enhances the localization of C–H correlations around 1.154 Å. These changes show that, under specific annealing conditions, only the H atoms change their configurations in a noticeable way. It follows that, in experiment, high-temperature annealing should be carried out only in hydrogen atmosphere to prevent hydrogen effusion and to reduce strain.

The H–H correlations in a-SiC:H are affected by large statistical errors associated with the very small number of H atoms in our sample. However, the peak revealed around 1.5 Å in the H–H PCF can be considered as attributable to small nearest-neighbour correlations between H atoms. This feature is enhanced by the annealing cycle. The a-SiC:H sample contains two sp C atoms (C–C–C configuration) and one C atom in the H–C–Si configuration. Correspondingly, the increase in the number of H atoms in the sample can lead to the formation of new C–H_3 bonds, and to an increase in the number of C–H and C–H_2 bonds, which can crucially modify the picture of H–H correlations.

The total DOS of a-SiC and a-SiC:H samples are presented in figure 2. The characteristic feature of both spectra is the absence of an ionicity gap around −11 eV. The latter is caused by the presence of about 50% of homonuclear bonds in the two alloys which gives rise to additional states in the ionicity BG region [9]. We note that the introduction of hydrogen in amorphous SiC weakly influences the chemical ordering. It is worth mentioning that our bonding picture for a-SiC is very similar to the one presented in [4], where about 45% of homonuclear bonds were found. Figure 2 clearly shows the tendency toward the formation of a BG around the Fermi energy (around +0.29 and −0.02 eV in a-SiC and as-quenched a-SiC:H, respectively). Because of a low content, hydrogen modifies the DOS insignificantly. In contrast to expected results, we do not observe an increase in the BG caused by hydrogenation [16]. This can be attributed to an increase in the number of coordination defects with hydrogenation. The

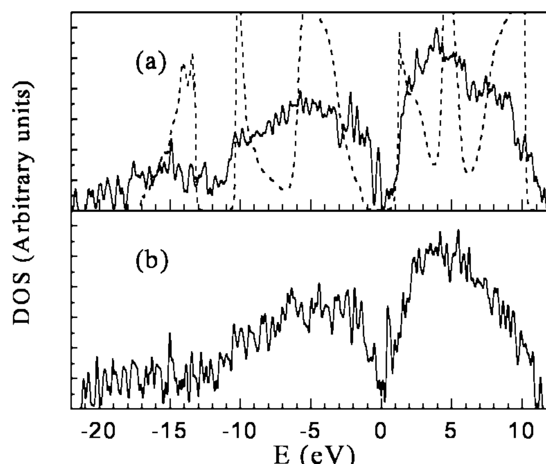

Figure 2. The calculated total DOS of: (a) a-SiC (solid curve) and 3C-SiC (dashed curve); (b) as-quenched a-SiC:H (solid curve).

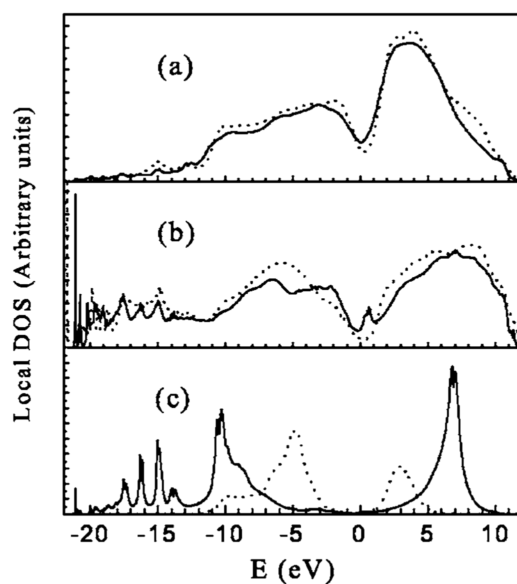

Figure 3. The calculated local DOS of a-SiC and as-quenched a-SiC:H: (a) Si atoms in a-SiC (dashed curve) and in a-SiC:H (solid curve); (b) C atoms in a-SiC (dashed curve) and in a-SiC:H (solid curve); (c) H atoms in Si–H bonds (dashed curve) and in C–H bonds (solid curve)

inspection of the local DOS for C–H and Si–H bonds shows that the distinct BG is only observed in the spectra of tetrahedrally coordinated atoms. Correspondingly, slow cooling or increasing in hydrogen content can lead to the broadening of a semiconducting gap.

As seen from figure 3, where the local spectra of Si, C, and H sites in a-SiC and a-SiC:H are shown, the general shapes of the local Si DOS in the two samples are similar, indicating similar short-range order around Si atoms. Two additional peaks around -1.5 and $+0.7$ eV appear in the C local spectrum of a-SiC:H. These peaks are not associated with hydrogenation, but instead with the appearance of C sp and sp^2 atoms in a-SiC:H. Hydrogen does not appreciably

influence the Si and C local electronic states because of its small mole fraction. The bonding Si–H and anti-bonding Si–H* states contribute to the DOS around −5 and +3 eV, respectively. A more complex picture is observed for the local DOS associated with the H atoms located near the C atoms. We identified C_s–H_s states below −13 eV, C_p–H_s states around −10 and −8 eV, and C_p–$H_s^\star$ states around +7 eV. Note that the two low-energy regions have several peaks caused by H–C bonds with different local environments. For example, in a-SiC:H, the H–C–Si_3, H–C–C_3, H–C–Si, H–C–CSi_2, H_2–C–CSi, and other configurations are present. The distributions obtained for Si–H and C–H states are consistent with both experimental and theoretical predictions [16]. The local DOS centred on the Si and C sites of Si–H and C–H bonds (not shown) give somewhat sharp peaks at the positions where the peaks of H DOS are also located.

4. Conclusion

A variant of the TB–MD method was proposed to generate a-SiC and a-SiC:H under conditions that mimic the experimental ones. The application of this approach enabled us to suggest a plausible model for the atomic and electronic properties of a-SiC:H. Although our picture of the inter-atomic interactions in a-SiC:H is generally consistent with previous theoretical models for a-C:H and a-Si:H and with experiment, peculiarities were found. Also, in contrast to experiment, no appreciable increase in the heteronuclear bonds due to hydrogenation has been observed. Finally it was suggested that chemical ordering was mostly determined by a cooling rate and the vapour structures.

Acknowledgments

This work was supported in part by STCU Contract Nos 1591 and 1590-C. The work of PT was performed under the auspices of US Department of Energy by the University of California Lawrence Livermore National Laboratory under Contract No W-7405-ENG-48.

References

[1] Bullot J and Schmidt M P 1987 *Phys. Status Solidi* b **143** 346
[2] Hamakawa Y 1998 *Renew. Energy* **15** 22
[3] Calcagno L, Martins R, Hallen A and Skorupa W (ed) 2001 *Amorphous and Microcrystalline Silicon Carbide: Materials and Applications* vol 112 (Amsterdam: European Materials Research Society)
[4] Finocchi F, Galli G, Parrinello M and Bertoni C M 1992 *Phys. Rev. Lett.* **68** 3044
[5] Kelires P C 1992 *Phys. Rev.* B **46** 10048
[6] Demichelis F, Giorgis F, Pirri C F and Tresso E 1996 *Physica* B **225** 103
[7] Desalvo A, Giorgis F, Pirri C F, Tresso E, Rava P, Galloni R, Rizzoli R and Summonte C 1997 *J. Appl. Phys.* **81** 7973
[8] Magafas L 1998 *J. Non-Cryst. Solids* **238** 158
[9] Ivashchenko V I, Shevchenko V I, Rusakov G V, Klymenko A S, Popov V M, Ivashchenko L A and Bogdanov E I 2002 *J. Phys.: Condens. Matter* **14** 1799
[10] Ivashchenko V I, Turchi P E A, Shevchenko V I, Ivashchenko L A and Rusakov G V 2002 *Phys. Rev.* B **66** 195201
[11] Vogl P, Hjalmarson H J and Dow J D 1983 *J. Phys. Chem. Solids* **44** 365
[12] Molteni C, Colombo L and Miglio L 1994 *Phys. Rev.* B **50** 4371
[13] Bockstedte M, Kley A, Neugebauer J and Scheffer M 1997 *Comput. Phys. Commun.* **107** 187
[14] Allen W D and Schaefer H F 1986 *Chem. Phys.* **108** 243
[15] Johnson B G, Gill P M W and Pople J A 1993 *J. Chem. Phys.* **98** 5612
[16] Robertson J 1992 *Phil. Mag.* B **66** 615
[17] Winn M D, Rassinger M and Hafner J 1997 *Phys. Rev.* B **55** 5364

[18] Buda F, Chiarotti G L, Car R and Parrinello M 1991 *Phys. Rev.* B **44** 5908

[19] Klein P, Urbassek H M and Frauenheim Th 1999 *Phys. Rev.* B **60** 5478

[20] Godwin P D, Horsfield A P, Stoneham A M, Bull S J, Ford I J, Harker A H, Pettifor D G and Sutton A P 1996 *Phys. Rev.* B **54** 15785

[21] Haydock R, Heine V and Kelly M J 1972 *J. Phys. C: Solid State Phys.* **5** 2845

[22] Nex C M M 1984 *Comput. Phys. Commun.* **43** 101